Nuclear Instruments and Methods in Physics Research B 365 (2015) 30–34

Contents lists available at ScienceDirect

Nuclear Instruments and Methods in Physics Research B

journal homepage: www.elsevier.com/locate/nimb

Structural modifications induced by ion irradiation and temperature in boron carbide B_4C

G. Victor [a,*], Y. Pipon [a,b], N. Bérerd [a,b], N. Toulhoat [a,c], N. Moncoffre [a], N. Djourelov [d,e], S. Miro [f], J. Baillet [a], N. Pradeilles [g], O. Rapaud [g], A. Maître [g], D. Gosset [h]

[a] Institut de Physique Nucléaire de Lyon (IPNL), Université Lyon 1, CNRS/IN2P3, 4 rue Enrico Fermi, 69622 Villeurbanne Cedex, France
[b] Institut Universitaire de Technologie (IUT) Lyon-1, Université Claude Bernard Lyon 1, 69622 Villeurbanne Cedex, France
[c] CEA-DEN, Saclay, 91191 Gif-sur-Yvette, France
[d] Institute for Nuclear Research and Nuclear Energy, Bulgarian Academy of Sciences, 72 Tzarigradsko chaussee blvd, BG-1784 Sofia, Bulgaria
[e] ELI-NP, IFIN-HH, 30 Reactorului Str, MG-6 Bucharest-Magurele, Romania
[f] CEA-DEN, Service de Recherches de Métallurgie Physique, Laboratoire JANNUS, F-91191 Gif-sur-Yvette, France
[g] SPCTS, UMR CNRS 7315, Centre Européen de la céramique, University of Limoges, France
[h] CEA, Saclay, DMN-SRMA-LA2M, 91191 Gif-sur-Yvette, France

ARTICLE INFO

Article history:
Received 1 October 2014
Received in revised form 13 April 2015
Accepted 15 July 2015
Available online 24 July 2015

Keywords:
Irradiation
Boron carbide
Structural defects
Slow positron
Raman

ABSTRACT

Already used as neutron absorber in the current French nuclear reactors, boron carbide (B_4C) is also considered in the future Sodium Fast Reactors of the next generation (Gen IV). Due to severe irradiation conditions occurring in these reactors, it is of primary importance that this material presents a high structural resistance under irradiation, both in the ballistic and electronic damage regimes. Previous works have shown an important structural resistance of boron carbide even at high neutron fluences. Nevertheless, the structural modification mechanisms due to irradiation are not well understood. Therefore the aim of this paper is to study structural modifications induced in B_4C samples in different damage regimes.

The boron carbide pellets were shaped and sintered by using spark plasma sintering method. They were then irradiated in several conditions at room temperature or 800 °C, either by favoring the creation of ballistic damage (between 1 and 3 dpa), or by favoring the electronic excitations using 100 MeV swift iodine ions ($S_e \approx 15$ keV/nm). Ex situ micro-Raman spectroscopy and Doppler broadening of annihilation radiation technique with variable energy slow positrons were coupled to follow the evolution of the B_4C structure under irradiation.

1. Introduction

Boron carbide is the third hardest naturally occurring material. This property makes B_4C very interesting in order to be used in armor and abrasive applications [1]. Other properties such as high neutron absorption cross sections (provided by ^{10}B), high melting temperature (around 2400 °C) and chemical stability at high temperature make boron carbide a good candidate as neutron absorber in nuclear power plants. This ceramic is currently widely used in the French pressurized water reactors and is foreseen for the fourth generation of nuclear reactors [2] in particular for the sodium-cooled fast reactor (SFR). This type of reactor is the most matured technology from the view point of industrial deployment while other 4th generation reactors as GFR (Gas Fast reactors) still require long term development before a test reactor project could begin [3]. That is the reason why, in France, CEA has launched in 2010, together with its industrial partners AREVA-NP and EDF, the project of a prototype reactor called ASTRID (Advanced Sodium Technical Reactor for Industrial Demonstration).

For this reactor, reactivity control of the core will be performed by two independent systems of boron carbide rods. These rods will: (i) control the evolution of the reactivity and, (ii) be dropped in case of emergency shutdown. At last, boron carbide will be used as upper and radial shielding of the reactor core. In fast neutron reactors of the fourth generation, the high neutron flux will lead to a more important damage rate of about 200 dpa and the operating temperature will range between 350 and 1200 °C. These conditions which are more critical than in Pressurized Water Reactors (PWR), will lead to a shorter lifetime for B_4C rods. Therefore it is

* Corresponding author at: IPNL, Bâtiment Paul Dirac, 4 rue Enrico Fermi, F-69622 Villeurbanne Cedex, France. Tel.: +33 4 72 43 10 57.
E-mail address: g.victor@ipnl.in2p3.fr (G. Victor).

http://dx.doi.org/10.1016/j.nimb.2015.07.082
0168-583X/

crucial to understand the behavior of B_4C and in particular the evolution of its structure in these extreme conditions.

Indeed, boron carbide, as many boron-rich compounds, has a complex structure widely studied since the 70's [4] that remains a hot topic nowadays [5–7]. In its idealized form, the structure of boron carbide is usually described in a rhombohedral unit cell (space group R-3m) that contains one icosahedral unit (mainly boron) and one linear 3-atoms chain (mainly carbon), corresponding to the ideal composition $B_{12}C_3$. The icosahedral units are composed of two distinct crystallographic sites called equatorial (noted "e") for the atoms linked to the central 3-atoms chains and polar (noted "p") for the atoms linked to the atoms of other icosahedra. Four sites are therefore available for a total of 15 boron and carbon atoms in the crystal structure. Thus the B and C atoms are interchangeable within both icosahedral and inter icosahedral atom chains. This constitutes the basis for the large homogeneity range for B–C system leading to structures as $(B_{11}C^p)$CBC or (B_{12})CCC.

Past researches have been performed on B_4C samples irradiated by neutrons, using techniques such as Raman and X-ray Diffraction in order to study the structural modifications induced by irradiation [8,9]. The results put forward a good resistance to irradiation attributed to the boron icosahedra which forms the B_4C structure and which can self-anneal under irradiation [10]. However the structural modifications of B_4C are still not fully understood and must be assessed in the framework of the SFR conditions.

In this study, we chose to shape and sinter B_4C pellets with controlled density and controlled elemental composition. These pellets were then irradiated either in ballistic regime to create dpa or by using swift heavy ions in order to enhance the electronic excitation part of irradiation. The structural evolution was studied before and after irradiation by combining two complementary techniques: micro-Raman spectroscopy which provides near surface information, whereas Position Annihilation Spectroscopy (PAS) with slow positrons gives information as function of depth.

2. Materials and methods

2.1. Sample preparation

HD20 boron carbide powder bought from H.C. Starck was shaped and sintered using the non-conventional Spark Plasma Sintering (SPS) method at the SPCTS Limoges (France). Two sintering conditions were experimented in order to obtain full dense sintered specimens. The powders were sintered in the form of cylinders (Ø = 10 mm and 5 mm thick) at two different temperatures (1750 °C and 1850 °C) under vacuum with an uniaxial applied load of 75 MPa during 5 min. The densities of the cylinder sintered in both conditions were measured by gas pycnometry. The relative densities were about 97–98% at 1750 °C and 99–100% at 1850 °C. Each sample was cut into two pellets of 2 mm thickness under water with a 1 mm thick diamond saw. Surfaces were mechanically polished with diamond paste of gradually reduced grain size (from 9 μm to 1 μm). After polishing the pellets were annealed a first time at 1000 °C during 10 h in a PECKLY© tubular furnace in order to degas the pellet surfaces, and a second time in an induction furnace at 1400 °C during 3 h to anneal the surface defects caused by polishing and reveal the microstructure. Both annealing were performed under a good secondary vacuum ($\sim 10^{-7}$ mbar). SEM microscopy observations showed samples with an important heterogeneity of grain size, from about 500 nm to almost 4 μm.

2.2. Sample irradiation

The irradiation conditions were chosen in order to favor either the ballistic damage (using 600 keV C^+ and 800 keV Ar^+) or the ionization effects due to electronic excitation (with 100 MeV iodine ions). Thus, the irradiations of the boron carbide pellets were performed either at the 4 MV Van de Graaff, the 400 kV IMIO accelerators at IPNL or the Tandem accelerator in Orsay. They were carried out using a specific cell developed at IPNL and allowing heating the samples at high temperature. This cell has been fully described by Marchand et al. [11]. Let us just remind that to ensure the sample heating, the sample holder consists in a pyrolitic boron nitride plate with an enclosed tungsten resistance able to heat the sample up to 1200 °C through Joule effect. AC thermocouple (Tungsten-5% Rhenium vs. Tungsten-26% Rhenium; 0–2320 °C) is used to measure the target temperature. Moreover, the sample surface temperature can be controlled with a bichromatic pyrometer. The whole set is encapsulated in stainless steel covered by a molybdenum layer to protect steel from temperature increase. The target holder is cooled down using water cooling tubes. Table 1 summarizes all the irradiation conditions of the boron carbide pellets. In Table 2 are gathered some parameters calculated by SRIM software [12] in order to quantify the damage issuing from the irradiation. The displacement energy thresholds used for the calculations are respectively of 28 eV and 25 eV for C and B.

2.3. Sample characterization

The structural evolution of the irradiated boron carbide sample was first studied by micro-Raman spectroscopy. Raman characterizations were carried out with a Renishaw Invia Reflex device equipped with a Leica DM2500 microscope (×100 objective) at the JANNUS laboratory in Saclay. Raman scattering measurements were performed using the 532 nm line of a frequency-doubled Nd–YAG laser with an output power of around 2 mW to avoid sample heating. The changes in defect concentration induced by irradiation were characterized by Doppler broadening of the annihilation gamma-line (DBAL), one of the PAS methods. The measurements were performed on the direct current slow positron beam (SPB) at INRNE-BAS, Sofia. The magnitude of the guiding magnetic field was increased from the usual 70 G to 100 G along the beam axis in order to keep the positron beam spot smaller than 5 mm in diameter. The DBAL measurements were carried out with a Canberra high purity Ge detector (HPGe) with a resolution of 1.17 keV (FWHM) at the 514 keV line of ^{85}Sr. The HPGe detector was set up at a distance of 4 cm from the sample perpendicular to the beam axis. The energy spectra were collected with statistics of $\sim 5 \times 10^5$ counts in the 511-keV peak region. For the DBAL analysis, the stepwise background of the Doppler broadened 511-keV peak was subtracted and the sharpness of the peak was characterized by a S parameter defined as the ratio of the central region counts ($|\Delta| < E_s = 0.92$ keV, where Δ is the shift from 511 keV) over the integrated counts in the peak (511 ± 10 keV). The positron implantation profile was taken as $P(z,E) = 2(z/z_0)\exp(-(z/z_0)^2)$ where $z_0 = 2z_m/\sqrt{\pi}\,E$ is the incident e^+ energy in keV, z in nm is the depth, and the mean penetration depth is determined by $z_m = (36/\rho)\,E^{1.62}$, the density ρ is in g cm^{-3} [13]. VEPFIT software was used to fit the $S(E)$ profiles [14]. One way of qualitative analysis of the DBAL results is to check the differences in S parameters from the reference sample as shown in Fig. 2. The plotted data

Table 1
Irradiations conditions.

Ions	Energy (MeV)	Flux (at.cm^{-2} s^{-1})	Fluence (at.cm^{-2})	Temperature
C^+	0.6	1×10^{12}	2×10^{16}	RT
Ar^+	0.8	2.7×10^{12}	1×10^{16}	RT
I^{9+}	100	1.2×10^{12}	5×10^{15}	RT/800 °C

Table 2
Irradiation parameters calculated with SRIM. For C^+ and $Ar^{+\cdot}$ ballistic damage is favored while electronic excitations predominate for I^{9+}.

Ions	Rp (μm)	Ballistic damages (dpa)	S_n (keV nm^{-1})	S_e (keV nm^{-1})
C^+	0.75	1–2	0.01	1.1
Ar^+	0.51	3–4	0.23	1.5
I^{9+}	11.4	~0	0.08	15

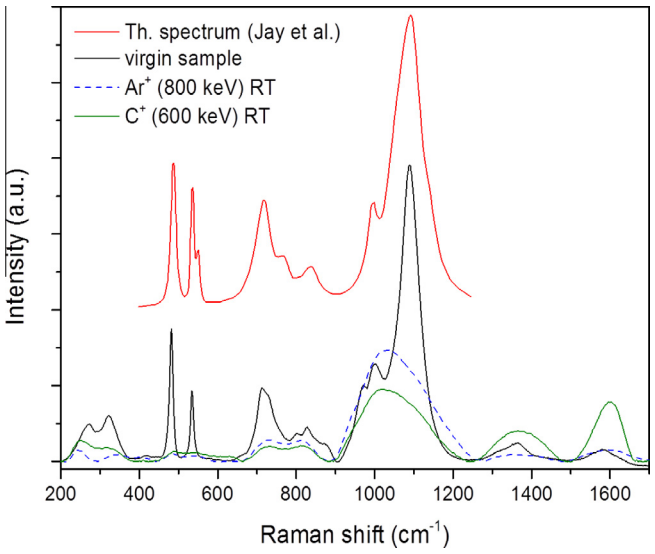

Fig. 1. Raman spectra of boron carbide samples: virgin, irradiated at RT with 600 keV C^+ and 800 keV Ar^+.

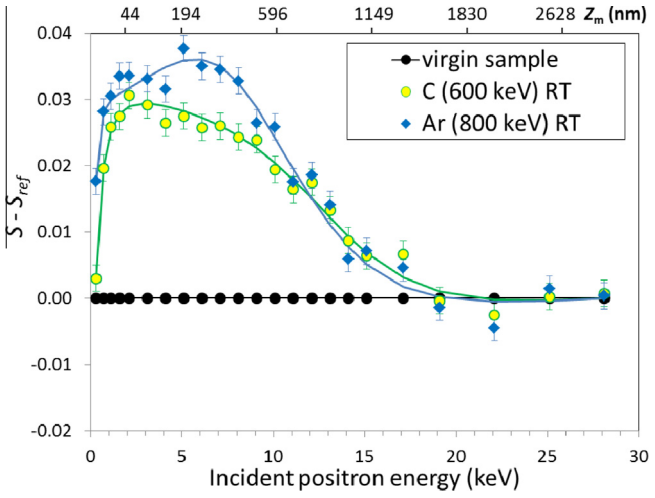

Fig. 2. Difference of the S parameter from the S parameter of the reference sample as a function of the incident positron energy E.

carry information on the defects (created or annealed) during the irradiation and annealing treatments. Further quantitative analysis of these data by VEPFIT is not possible due to the subtraction of *S* parameter of the reference thus masking the positron diffusion lengths; however, rough estimation of the defects profile (see Fig. 3) is still possible. Finally, to observe the surface modification on the sample, Scanning Electron Microscopy (SEM) was performed on the boron carbide at CTμ (France). The surfaces were observed with an acceleration voltage of electrons of 5 kV using a FEI Quanta 250 FEG.

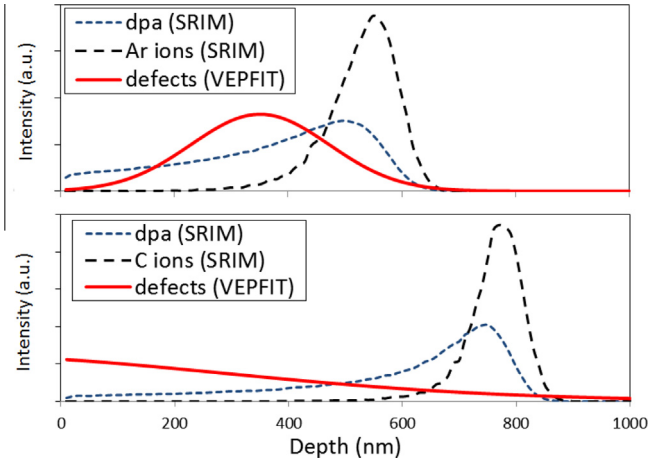

Fig. 3. Depth distributions and displacement per atom (dpa) calculated by SRIM and of defects obtained by VEPFIT analysis.

3. Results and discussion

3.1. Virgin sample

The Raman spectra of boron carbide are characterized by a series of bands extending from 200 to 1200 cm^{-1}. Let us look at the virgin sample spectrum and compare it with recent results obtained by Jay et al. [6]. Fig. 1 displays the spectrum of the virgin sample which exhibits the typical Raman modes of the B_4C structure. It is in very good agreement with the theoretical Raman spectrum calculated by Jay et al.[6]. Similar main Raman shifts are found on both spectra: (i) at 481 and 543 cm^{-1}, two modes representing quasi-degenerate harmonic E_g modes with atomic motions characterized by the rotation of the chains and the libration of the icosahedra respectively, (ii) at 1089 cm^{-1} (1095 cm^{-1} in the calculations), the A_{1g} mode characteristic of the symmetric chain stretching. Moreover, because of amorphous/graphitic carbon inclusions commonly present in commercial boron carbide, Raman spectra show the characteristic D and G bands at respectively 1359 and 1577 cm^{-1} [15].

3.2. Ballistic damage

To study the impact of the nuclear slowing down process, irradiations at low energy with C^+ and Ar^+ were carried out at RT, leading to a number of displacements per atom (dpa, as estimated with the SRIM software) of 1–2 for C^+ and 2–3 for Ar^+ at depths of respectively 700 nm and 500 nm (cf Table 2). In Fig. 1 are also represented the Raman spectra recorded for the RT irradiated B_4C samples with 800-keV Ar ions or 600 keV C ions. The Raman spectra of irradiated samples show that in both irradiation conditions, a collapsing of the modes representative of the B_4C structure occurs, due to an important local disorder of the structure. It is worth noting that since all the modes are damaged, the analysis is limited to the damaged material with no contribution of the bulk.

This analysis was completed by characterization of DBAL spectra obtained with variable energy slow positrons. Differences in $S(E)$ depth profiles from the reference sample are displayed in Fig. 2. This figure underlines the effect due to the evolution of the vacancy concentration as a function of depth (or incident positron energy) for the irradiated samples. The dots stand for the measurements and the lines for the fit made with VEPFIT after a DBAL analysis (assuming a Gaussian shape of the concentration of the defects). As expected, defects are created within a 800 nm range

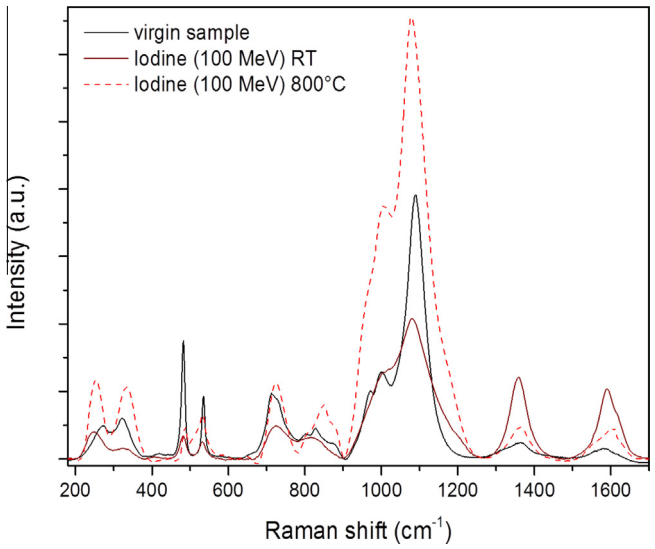

Fig. 4. Raman spectra of boron carbide samples: virgin, irradiated with 100 MeV iodine ions at RT and 800 °C.

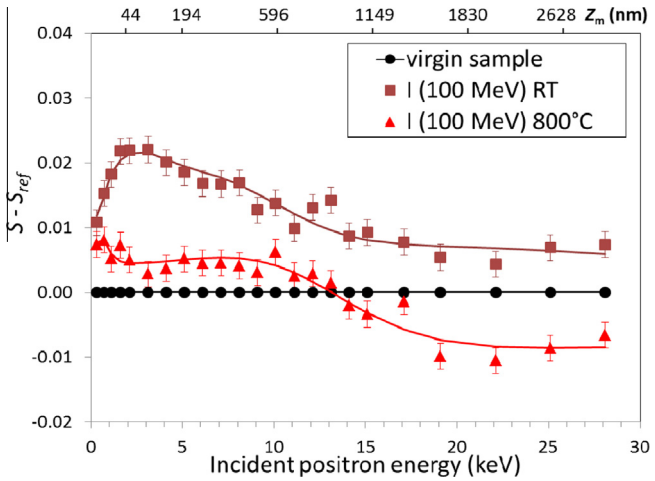

Fig. 5. Difference of the S parameter from the S parameter of the reference sample as a function of the incident positron energy E.

in both irradiation conditions. This range is of the same magnitude of the one calculated by SRIM for the defect region.

The defect profiles obtained by DBAL analysis are shown in Fig. 3 together with the dpa and ion distributions given by SRIM. In general, positrons are not very sensitive to interstitial defects if these defects are neutral or positively charged which was confirmed in our previous studies on Xe-implanted ZrC and UO_2 [16,17]. Such a situation is seen in Fig. 3(top) for the Ar-implanted sample where the defect depth profile agrees satisfactory with the calculated by SRIM dpa distribution. However, Fig. 3(bottom) for C-implanted sample shows a completely different picture. Defects at the projection range of the implanted C are not detected. This is due to the fact that C is a structural element of the boron carbide. Indeed, the atomic displacements result in the creation of vacancies but these vacancies are efficiently compensated by the implanted C, with a concentration of 1.4 at.% at the implantation peak according to SRIM simulations, and only vacancies close to the surface survive. This result is complementary to that obtained by Raman on the C^+ irradiated sample showing an increase of amorphous and graphitic carbon D and G bands.

3.3. Electronic excitations and temperature

To evaluate the impact of the electronic slowing down process and of temperature, irradiations were performed using 100 MeV iodine ions at RT and at 800 °C (cf. Table 1). Micro-Raman spectroscopy and PAS analyses were also performed on these samples. Fig. 4 displays the Raman spectra recorded before and after iodine irradiation. It shows that the peaks are broader and flattened for the sample irradiated at RT compared to the virgin sample. This means that electronic excitations increase the local disorder in the structure. This was previously observed in the case of ballistic damage, but with a larger impact. At 800 °C, we observe a narrowing of the peaks in comparison with the peaks of the RT irradiated sample. This observation probably means that a structural restructuration occurs at this temperature.

Again, PAS analysis brings complementary results. The PAS spectra are displayed in Fig. 5. It is important to remind that the 100-MeV iodine ions penetrate much deeper (11 μm) than the 30-keV positrons. Therefore with positrons the irradiation effects can only be studied within a depth of 2 μm. As seen from the data shown in Fig. 5, the RT irradiation results in higher *S* parameter compared to the reference. This means that positron traps are created and most probably these traps are vacancies. By maintaining the sample temperature during the I-irradiation at 800 °C, the vacancies created by the irradiation are successfully annealed and even the heat-treatment improves the bulk structure of the sample as seen from the negative difference with the reference sample.

Fig. 6 displays the SEM micrographs obtained on the virgin and iodine irradiated samples at RT and 800 °C. The virgin sample (Fig. 6a) presents a smooth surface with little porosity only located at the grain boundaries. For the sample irradiated at 800 °C (Fig. 6b), the surface morphology looks similar except an increase

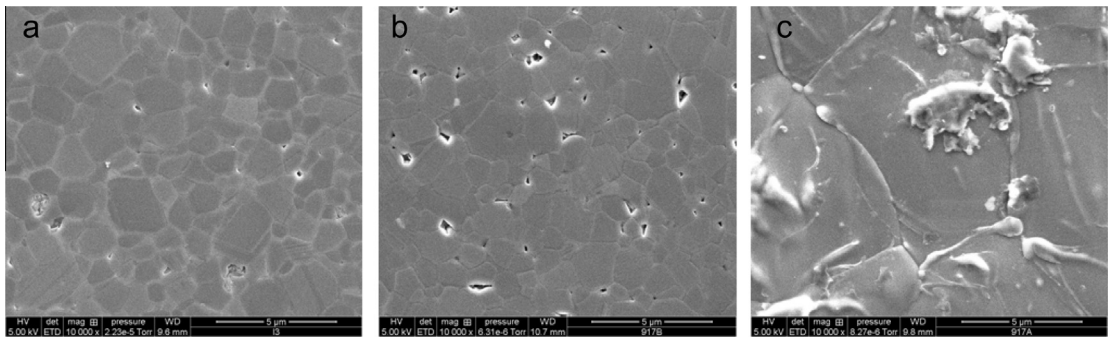

Fig. 6. SEM images displaying the surface morphology of boron carbide samples before (a) and after irradiation with 100 MeV iodine ions at 800 °C (b) and RT (c).

of open pores at grain boundaries. This may be caused by the desorption of CO and CO_2 species resulting from the presence of free graphite trapped as graphite inclusions at the grain boundaries [18] and of oxygen, whose presence was confirmed by nuclear reaction analysis (not shown in the present article), near the surface of the samples (around 0.5 at.% in the first 100 nm). Indeed, during B_4C elaboration, at high temperature, a part of carbon does not react and remains in the form of free carbon. Moreover, the cooling from elevated temperatures to room temperature during the sintering process may not be slowed down enough to allow the excess carbon to completely separate out from B_4C matrix. For the sample irradiated at RT (Fig. 6c), an important deformation and expansion of the grains occurs and blisters appear on the grain surfaces.

4. Conclusion

The results obtained by both techniques, DBAL with slow positrons and micro-Raman spectroscopy, show the interest of coupling these techniques for damage study. In case of ballistic damages, our results are in good agreement with those obtained by Gosset et al. [19] on samples irradiated at 4 dpa. Indeed Raman spectra are quite similar indicating a B_4C local disorder of the same order.

For electronic excitations, SEM images of the sample irradiated at RT evidence deformation, expansion and blistering of the grains. At 800 °C, the grain size does not change but an increase of open porosity at grain boundaries is observed. One of the hypothesis to explain this observation is the presence of free carbon and oxygen in the samples, possibly leading to the formation of CO and CO_2 under irradiation at 800 °C.

Finally these results are a good example of competition between restructuration induced by temperature and disordering induced by irradiation.

Acknowledgements

The authors would like to thank the IPNL accelerator team and the Orsay Tandem staff for their efficient help during the irradiation runs. This work is supported by the collaborative NEEDS project.

References

[1] F. Thévenot, J. Eur. Ceram. Soc. 6 (1990) 205–225.
[2] G. Locatelli, M. Mancini, N. Todeschini, Energy Policy 61 (2013) 1503–1520.
[3] Y. Sakamoto, J. Rouault, C. Grandy, T. Fanning, R. Hill, Y. Chikazawa, S. Kotake, Nucl. Eng. Des. 254 (2013) 194–217.
[4] H.L. Yakel, Acta Crystallogr. B31 (1975) 1797–1806.
[5] K. Shirai, S. Emura, J. Solid State Chem. 133 (1997) 93–96.
[6] A. Jay, N. Vast, J. Sjakste, O. Hardouin Duparc, Appl. Phys. Lett. 105 (2014) 031914, http://dx.doi.org/10.1063/1.4890841.
[7] A. Ektarawong, L. Hultman, J. Birch, B. Alling, Phys. Rev. B 90 (2014) 024204, http://dx.doi.org/10.1103/PhysRevB.90.024204.
[8] D. Simeone, D. Gosset, D. Quirion, X. Deschanels, J. Nucl. Mater. 264 (1999) 295–308.
[9] D. Simeone, C. Mallet, P. Dubuisson, G. Baldinozzi, C. Gervais, J. Maquet, J. Nucl. Mater. 277 (2000) 1–10.
[10] M. Carrard, D. Emin, L. Zuppiroli, Phys. Rev. B 51 (1995) 11270–11274.
[11] B. Marchand, N. Moncoffre, Y. Pipon, N. Bérerd, C. Garnier, L. Raimbault, P. Sainsot, T. Epicier, C. Delafoy, M. Fraczkiewicz, C. Gaillard, N. Toulhoat, A. Perrat-Mabilon, C. Peaucelle, J. Nucl. Mater. 440 (2013) 562–567.
[12] J.F. Ziegler, M.D. Ziegler, J.P. Biersack, Nucl. Instr. Meth. Phys. Res. Sect. B 268 (2010) 1818–1823.
[13] A. Vehanen, K. Saarinen, P. Hautojarvi, H. Huomo, Phys. Rev. B 35 (1987) 4606.
[14] A. Van Veen, H. Schut, M. Clement, J.M.M. de Nijs, A. Kruseman, M.R. Ijpma, Appl. Surf. Sci. 85 (1995) 216–224.
[15] V. Domnich, S. Reynaud, R.A. Haber, M. Chhowalla, J. Am. Ceram. Soc. 94 (2011) 3605–3628.
[16] N. Djourelov, G. Gutierrez, H. Marinov, E. Popov, N. Toulhoat, N. Moncoffre, Y. Pipon, Nucl. Instr. Meth. Phys. Res. Sect. B 269 (2011) 2709–2714.
[17] N. Djourelov, B. Marchand, H. Marinov, N. Moncoffre, Y. Pipon, P. Nédélec, N. Toulhoat, D. Sillou, J. Nucl. Mater. 432 (2013) 287–293.
[18] T. Inoue, T. Onchi, H. Kôyama, H. Suzuki, J. Nucl. Mater. 74 (1978) 114–122.
[19] Dominique Gosset, Sylvie Doriot, Guillaume Victor, Vianney Motte, Nucl. Instr. Meth. Phys. Res. Sect. B (2014).